Journal Pre-proof

Supercritical CO_2 extraction of *V. vinifera* leaves: influence of cosolvents and particle size on removal kinetics and selectivity to target compounds

Marcelo M.R. de Melo, Benedict Carius, Mário M.Q. Simõ es, Inês Portugal, Jorge Saraiva, Carlos M. Silva

PII: S0896-8446(20)30210-2

DOI: https://doi.org/10.1016/j.supflu.2020.104959

Reference: SUPFLU 104959

To appear in: *The Journal of Supercritical Fluids*

Received Date: 18 May 2020

Revised Date: 22 June 2020

Accepted Date: 23 June 2020

Please cite this article as: de Melo MMR, Carius B, Simõ es MMQ, Portugal I, Saraiva J, Silva CM, Supercritical CO_2 extraction of *V. vinifera* leaves: influence of cosolvents and particle size on removal kinetics and selectivity to target compounds, *The Journal of Supercritical Fluids* (2020), doi: https://doi.org/10.1016/j.supflu.2020.104959

This is a PDF file of an article that has undergone enhancements after acceptance, such as the addition of a cover page and metadata, and formatting for readability, but it is not yet the definitive version of record. This version will undergo additional copyediting, typesetting and review before it is published in its final form, but we are providing this version to give early visibility of the article. Please note that, during the production process, errors may be discovered which could affect the content, and all legal disclaimers that apply to the journal pertain.

© 2020 Published by Elsevier.

Journal Pre-proof

Supercritical CO_2 extraction of *V. vinifera* leaves: influence of cosolvents and particle size on removal kinetics and selectivity to target compounds

Marcelo M.R. de Melo[1], Benedict Carius[1,2], Mário M.Q. Simões[3], Inês Portugal[1], Jorge Saraiva[3], Carlos M. Silva[1]*

[1] CICECO – Aveiro Institute of Materials, Department of Chemistry, University of Aveiro, Aveiro, Portugal;
[2] University of Applied Sciences, Department of Chemical Engineering and Biotechnology, 64295 Darmstadt, Germany;
[3] QOPNA & LAQV-REQUIMTE, Department of Chemistry, University of Aveiro, 3810-193 Aveiro, Portugal.

*Corresponding author: Tel.: + 351 234 401549; Fax: + 351 234 370084
E-mail address: carlos.manuel@ua.pt

Graphical Abstract

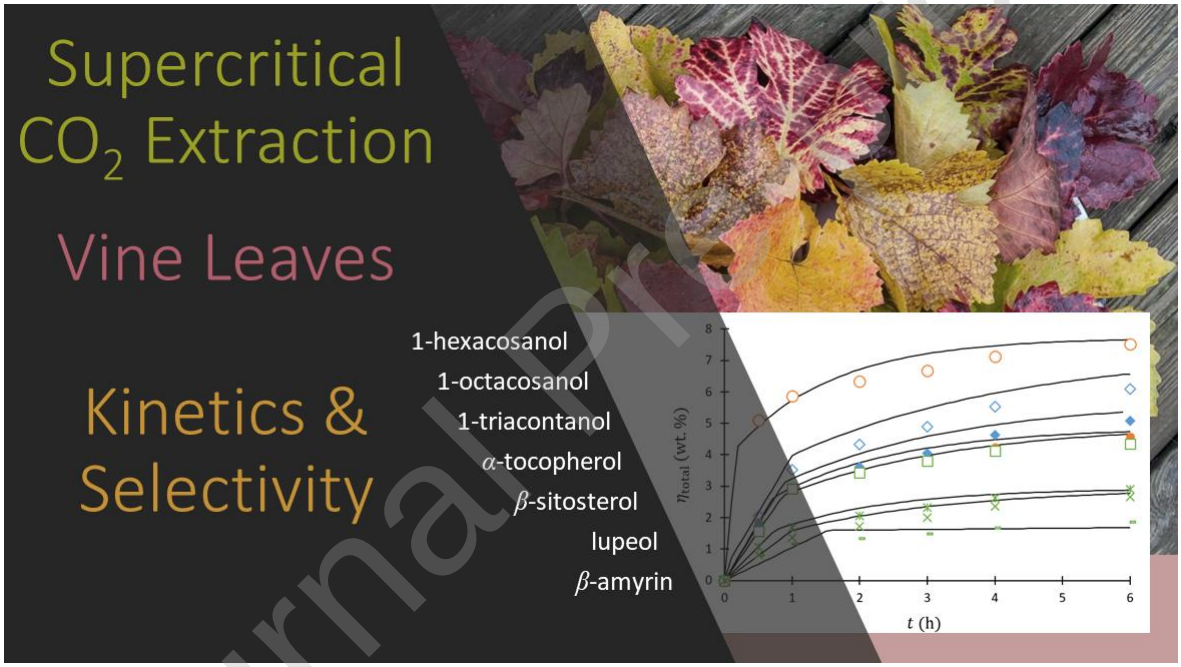

Highlights

- Measurement and modeling of SFE curves from *V. vinifera* leaves;
- Relevant extractives are long chain aliphatic alcohols, α-tocopherol, β-sitosterol, and triterpenes;
- Influence of CO_2 cosolvents and particle size upon SFE kinetics and selectivity;
- Results comprise 40 experimental SFE curves, modeled using broken plus intact cells model;

Journal Pre-proof

- Remarkable selectivities were obtained for triterpenes (lupeol and β-amyrin).

Abstract

Leaves from *Vitis vinifera* L. contain potential bioactive compounds, namely: long chain aliphatic alcohols (*e.g.*, 1-hexacosanol, 1-octacosanol and 1-triacontanol), α-tocopherol, β-sitosterol, and the triterpenes *β*-amyrin and lupeol. Supercritical fluid extraction (SFE) runs were measured at lab scale using: crushed and ground biomass; pure CO_2 at 300 bar and 40-80 ºC; and CO_2 modified with 5 and 10 wt.% of ethanol or ethyl acetate. Total SFE yields ranged from 1.86 to 7.52 wt.%. The broken plus intact cells model (BICM), provided a good fitting of the SFE curves with 4.06 % error for total yield and 1.98-5.49 % for the individual yields of the said compounds. The BICM results revealed that the SFE is limited by intraparticle diffusion. Remarkable experimental and calculated selectivities were obtained for triterpenes (lupeol and β-amyrin), starting with a score of 1.7 and increasing along time to 10-100.

Keywords: BIC Modeling, GC-MS, Soxhlet Extraction, Supercritical Fluid Extraction, Vine Leaves

1. Introduction

Among the high-volume agricultural crops farmed in Europe, grape vine (*Vitis vinifera* L.) is one of the most important species. Since the fruit (grape) is extensively explored for wine production, by-products (roots, stalks, bark and leaves) are inherently produced in huge amounts. For example, in Europe, 6.2 million hL of wine were produced in 2015 [1] leaving behind 14.5 million tons of waste [2].

Vine leaves are one of the least investigated by-products and are generally considered organic wastes. However, previous works addressing the composition of the extracts of *V. vinifera* leaves identified several compounds with possible economic interest. For instance, Fernandes *et al*. [3] showed that ethanolic extracts of grape leaves are rich in phenolic compounds with biological activity, mainly hydroxycinnamic acid derivatives and quercetin glycosides. Pensec *et al*. [4] focused on triterpenoids extracted with chloroform, namely, *β*-amyrin, lupeol, taraxerol, α-tocopherol and *β*-sitosterol. For example, α-tocopherol is a liposoluble antioxidant belonging to the Vitamin E class and is important

Journal Pre-proof

for protecting biological membranes (such as cell walls) [5]. β-sitosterol is an anticholesteremic drug and also an antioxidant [6]. As for the triterpenes, lupeol is a known bioactive compound used to treat cancer and malaria [7], β-amyrin (a precursor of oleanolic acid) exhibits antinociceptive and anti-inflammatory properties [8], and taraxerol evidences anti-inflammatory properties [9].

Supercritical fluid extraction (SFE) is a mature high-pressure technology that in most cases relies on carbon dioxide (CO_2) as the working solvent [10,11]. For the particular case of SFE of *V. vinifera* biomass, the solvent can be synergistically obtained from fermentative processes (*e.g,* wine production [12]), which adds value to the universal advantages of this technology, namely the preservation of the natural label on ensuing products due to the innocuousness of the CO_2, mild critical conditions ($T_c = 31.1$ ºC and $P_c = 73.8$ bar), the null solvent surface tension and inertness, and the dismissal or reduction of distillation/drying units to isolate the extract from the solvent and both from the exhausted solid matrix. The last decades have been marked by prolific research activity on natural extracts produced by SFE from plants such as aloe vera [13,14], cork [15,16], eucalypt [17,18], hemp [19,20], water hyacinth [21,22], stevia [23,24], and many others [25–28]. The most important operating conditions/parameters under investigation have been pressure, temperature, flow rate, cosolvent type and concentration, particle size, and extraction time [28]. The usual responses are total extraction yield, specific/individual yields (of molecules or families of molecules), concentration of target compounds in the extracts, and much more rarely selectivities [16,28]. An important variable influencing selectivity is frequently cosolvent type and/or concentration, which leads to a trade-off between higher total yields and individual yields of target compounds [16,29,30].

The SFE of grape seeds has been a hot investigation topic devoted to bulk vegetal oil [31–35], phenolics [36], flavonols [37] or phytosterols [38]. In this work, SFE technology was used for the first time to investigate natural extracts of leaves from *Vitis vinifera* L. The novelty of the study also encompasses the mapping of selectivity profiles for different target compounds and the identification of conditions for kinetic enhancement of the process. The influence of green cosolvents addition (ethanol and ethyl acetate) at two concentration levels, biomass particle size and temperature is accomplished and analysed using the broken plus intact cells model.

Journal Pre-proof

2. Materials & Methods

2.1 Chemicals

Carbon dioxide (CO_2, purity 99 %) was supplied by Air Liquide (Algés, Portugal). Dichloromethane (DCM, purity 99.9 %) and ethanol (E, purity 99.5 %) were supplied by Fisher Scientific (Leicestershire, United Kingdom). Ethyl acetate (EA, purity 99.9 %) was purchased from VWR International (Fontenay-sous-Bois, France). The chemicals used for silylation (preparation of samples for the GC-MS analysis – [39]) were pyridine (purity 99 %), *N*,*O*-Bis(trimethylsilyl)-trifluoroacetamide (purity 99 %) and trimethylsilyl chloride (purity 99 %), all purchased from Aldrich (United States). GC-MS calibration standards of ursolic acid, betulinic acid and oleanolic acid (purity > 98 %) were purchased from AK Scientific (Canada) and squalene (purity 99 %) was purchased from Aldrich (United States).

2.2 Biomass samples

Grape leaves from *Vitis vinifera* L. were collected on a vineyard located in the region of Amarante, Portugal (41º17'14.9"N 7º59'08.1"W) in October 2018, one week after the grape harvest season. The leaves were air dried at 30 °C and divided in two lots (see Figure 1), one comprising hand crushed pieces (d_p< 10 mm) and the other fine particles (d_p< 1 mm) obtained by grinding the leaves in a standard coffee grinder. Until further use, the samples were stored under dry and dark conditions at room temperature to prevent degradation. The leaves residual moisture (11.70 ± 0.26 wt.%) was determined by drying at 70 °C during 48 h, and the density (ρ_{Solid} = 1449 ± 24 kg m^{-3}) was measured by helium gas pycnometry (Quantachrome Instruments).

Journal Pre-proof

Journal Pre-proof

Figure 1 – Photos of crushed (left) and ground (right) leaves of *Vitis vinifera* L.

2.3 Soxhlet extraction

Soxhlet extractions (Sox) with dichloromethane (DCM), ethanol (E) and ethyl acetate (EA) were performed with 40 mL cartridges during 6 h, using 160 mL of solvent placed in a 250 mL round-bottomed flask. The sample cartridge was filled with the leaves (2.0 ± 0.1 g) and then sealed with a cotton wool plug.

Table 1 - Experimental conditions for the Soxhlet extractions of leaves (*V. vinifera*).

Soxhlet run	d_p (mm)	Solvent	T_{eb} * (°C)	t (h)
Sox DCM-G	< 1	Dichloromethane	39.6	6
Sox DCM	< 10	Dichloromethane	39.6	6
Sox EA	< 10	Ethyl acetate	76.9	6
Sox E	< 10	Ethanol	78.4	6

* normal boiling point of pure solvent ([40]); Sox, Soxhlet; DCM, dichloromethane; G, ground biomass; EA, ethyl acetate; E, ethanol.

Journal Pre-proof

2.4 Supercritical fluid extraction

Supercritical fluid extractions (SFE) were performed in a cylindrical 0.5 L lab scale extractor (7.3 cm of internal diameter, 12 cm of height), model Spe-ed™, from Applied Separations Inc. (USA), whose scheme is depicted in Figure 2. The cooled CO_2 (liquid stream) was pressurized using a liquid pump (diaphragm pump), and heated to the desired temperature in the pre-heating vessel. After reaching the $P - T$ setpoint conditions the dynamic extraction was started by opening the back pressure valve (labelled as 'regulator valve' in Figure 2). The SCF was fed to the bottom of the extraction bed and percolated the vegetal biomass. The outlet stream was depressurized in a cooled extract collector, and the expanded fluid was bubbled in ethanol to avoid the dragging the extract by the gaseous CO_2. Finally, ethanol was removed from the extracts by evaporation in a rotary evaporator until dryness. A calibrated HPLC pump was used to feed the cosolvent (if necessary) to a mixture point placed before the inlet of the extraction bed. At the end of the experiment the cosolvent was also removed by evaporation in a rotary evaporator until dryness.

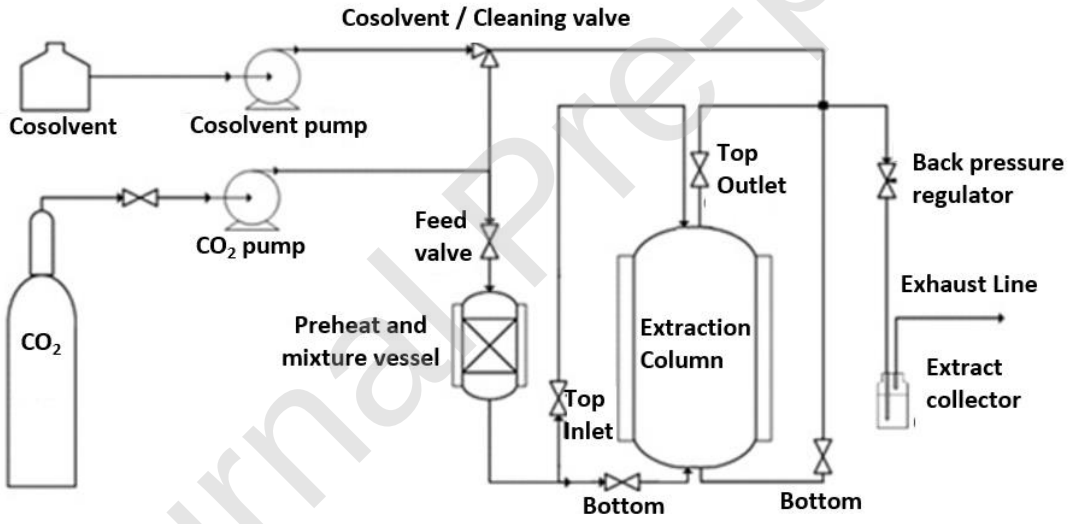

Figure 2 - Scheme of the lab-scale extraction unit – modified from [41,42].

Cumulative extraction curves were measured using six points per curve for the following extraction times: 0.5, 1, 2, 3, 4 and 6 h. In this work eight SFE curves were obtained for crushed (d_p< 10 mm) and ground (d_p< 1 mm) particles at three different temperatures (40, 60, 80 ºC). The extraction pressure and the supercritical CO_2 (SC-CO_2) flow rate were held constant at 300 bar and 12 g min^{-1}, respectively. The cosolvents applied to ground particles

Journal Pre-proof

were ethanol (E) and ethyl acetate (EA), with concentrations of 5 and 10 wt.% in relation to the constant SC-CO_2 flow rate. The option to use these cosolvents is owed to their innocuousness (compatible with food, cosmetics and pharma applications) and to the fact they can improve the affinity of the supercritical phase to more polar compounds. Contents of 0, 5 and 10 wt.% of cosolvent are usually adopted in the literature [28] and allow us to unveil its effect. Table 2 summarizes the SFE runs, where the following labels were adopted: B#, assay number #; G, ground biomass; EA or ea, ethyl acetate; E or e, ethanol.

The densities of the supercritical solvent system, ρ_{SCF}, were obtained from the works of Pitzer and Schreiber [43] (for pure CO_2), Pöhler and Kiran [44] and Kato *et al.* [45] (for CO_2 + E), and Falco and Kiran [46] (for CO_2 + EA). In turn, the reported bed densities (ρ_b) were determined by measuring the volume occupied by a known mass of biomass particles packed in a cylindrical vessel of known volume.

Table 2 - Experimental conditions for SFE extractions of leaves ($P = 300$ bar).

Run label	Cosolvent	T (°C)	d_p (mm)	ρ_b ($kg\ m^{-3}$)	ρ_{SCF} ($kg\ m^{-3}$)
B1	-	40	< 10	80	910.6 [43]
B2	-	60	< 10	80	830.5 [43]
B3	-	80	< 10	80	746.2 [43]
B4G	-	80	< 1	280	746.2 [43]
B5Ge5	5 wt.% E	80	< 1	280	769.7 [44,45]
B6Ge10	10 wt.% E	80	< 1	280	778.0 [44,45]
B7Gea5	5 wt.% EA	80	< 1	280	774.0 [46]
B8Gea10	10 wt.% EA	80	< 1	280	794.0 [46]

B#, assay number #; G, ground biomass; EA or ea, ethyl acetate; E or e, ethanol.

2.5 Gas chromatography–mass spectrometry (GC-MS) analysis

The GC-MS analysis of the extracts was done using a Shimadzu GCMS-QP2010 Ultra system equipped with a DB1-ms column (30.0 m × 0.25 mm × 0.25 μm film thickness, Agilent, USA) using the electron ionization mode operated at 0.1 kV. Helium was used as carrier gas at 1.18 mL min^{-1}. The GC injector temperature was set to 280 °C, the split ratio was 50, and the injection volume was 1 μL. The mass spectrometer ion source temperature was set to 250 °C and the interface temperature to 300 °C. The temperature program of the GC oven was as follows: 80 °C for 5 min, then ramped to 150 °C at 10 °C min^{-1}, then

Journal Pre-proof

increased to 300 °C at 3 °C min^{-1}, and finally held at 300 ºC for 30 min. The total runtime was 92 min. The reported results are the average of two injections, being more injections made whenever concordant values on the two initial injection were not found.

Prior to each GC-MS analysis, an aliquot of 20 mg of extract and 1 mg of tetracosane (internal standard) was silylated by adding 250 μL pyridine, 250 μL *N,O*-Bis(trimethylsilyl)trifluoroacetamide and 50 μL trimethylsilyl chloride, following a procedure described in the literature [47]. The sealed tubes were placed in a water bath, at T = 70 °C, during 30 to 60 min. Identification of the compounds was done by comparing the results to MS libraries (NIST 2014, NIST 2008 and WILEY 2007) and to the standard compounds (ursolic, betulinic and oleanolic acids). According to the chosen GC-MS method, the retention times of the 8 main compounds identified in this study were the following: 42.2 min (squalene), 45.5 min (1-hexacosanol), 48.9 min (α-tocopherol), 49.5 min (1-octacosanol), 52.4 min (β-amyrin), 52.6 min (β-sitosterol), 53.2 min (lupeol) and 53.5 min (1-triacontanol).

2.6 Phenomenological modeling

The broken plus intact cells model (BICM) was originally proposed by Sovová *et al.* [48,49] and comprises a mechanistic approach to explain the extraction of milled vegetal matrices using supercritical fluids, namely by acknowledging the occurrence of two distinct types of cellular structures: external cells with broken walls contacting with the supercritical fluid (mass transfer ruled by convection) and inner intact cells where diffusion prevails. It is the most used model within the research field [28]. In brief, BICM describes SFE of vegetal biomass based on kinetics, thermodynamics, and matrix related parameters. The extraction of compounds trapped inside vegetal cells (either broken or intact) into a supercritical fluid (SCF) phase can be described by the following sequential steps: (*i*) impregnation of the vegetal matrix and solubilisation of the solutes in the SCF phase; (*ii*) diffusion of the solubilized solutes from the intact cells to the broken cells; and (*iii*) diffusion of the solutes from the broken cells to the bulk SCF phase.

According to the BICM, SFE curves can be divided in three extraction periods [49]. The first is the constant extraction rate (CER) period, where solubilisation and external transport from the broken cells to the bulk are dominant. The second is the falling extraction rate (FER) period in which extraction relies also on more inaccessible regions,

Journal Pre-proof

namely intact cells, and so the rate is lower than in the CER period due to intraparticle resistance. The third and last branch is the diffusion-controlled (DC) period where usually only small amounts of extract are generated due to the prevalence of slow internal diffusion.

Adopting the integrated form of BICM, the cumulative weight (w) of extracts obtained in the three extraction periods is given by [49]:

$$w = Q_{\mathrm{CO_2}} y^{*}\, t\, [1 - \exp(-Z)] \qquad \text{for } 0 \le t \le t_{\mathrm{CER}} \tag{1}$$

$$w = Q_{\mathrm{CO_2}} y^{*}\, [t - t_{\mathrm{CER}} \exp(Zm(t) - Z)] \qquad \text{for } t_{\mathrm{CER}} \le t \le t_{\mathrm{FER}} \tag{2}$$

$$w = w' \left\{ X_0 - \frac{y^{*}}{W} \ln \left[1 + \left(\exp\left(\frac{W X_0}{y^{*}} \right) - 1 \right) \exp\left(\frac{W Q_{\mathrm{CO_2}}}{w'} (t_{\mathrm{CER}} - t) \right) \mathrm{g} \right] \right\} \qquad \text{for } t \ge t_{\mathrm{FER}} \tag{3}$$

where t_{CER} and t_{FER} represent the duration of the CER and FER periods, respectively. These equations are complemented by the following expressions:

$$Z = \frac{k_{\mathrm{f}} a\, w' \rho_{\mathrm{CO_2}}}{Q_{\mathrm{CO_2}} \rho_{\mathrm{b}}} \tag{4}$$

$$W = \frac{w' k_{\mathrm{s}} a}{Q_{\mathrm{CO_2}} (1 - \varepsilon_{\mathrm{b}})} \tag{5}$$

$$t_{\mathrm{CER}} = \frac{(1 - g) w' X_0}{Q_{\mathrm{CO_2}}\, y^{*} Z} \tag{6}$$

$$t_{\mathrm{FER}} = t_{\mathrm{CER}} + \frac{w'}{W Q_{\mathrm{CO_2}}} \ln \left[g + (1 - g) \exp\left(\frac{W X_0}{y^{*}} \right) \right] \tag{7}$$

$$Zm\,(t) = \frac{Z y^{*}}{W\, w'} \ln \left\{ \frac{1}{1 - g} \left[\exp\left(\frac{W Q_{\mathrm{CO_2}}}{w'} (t - t_{\mathrm{CER}}) \right) - g \right] \right\} \tag{8}$$

Journal Pre-proof

where t (h) is the extraction time, w (kg) is the cumulative mass of extract, w' (kg) is the weight of biomass in solute-free basis, ρ_{b} (kg m^{-3}) is the bed density, y^* is the solutes (pseudo-component) solubility in the supercritical phase, $Q_{\mathrm{CO_2}}$ (kg h^{-1}) is the mass flow rate of CO_2, ρ_{SCF} (kg m^{-3}) is the density of the supercritical fluid, ε_{b} is the bed porosity (obtained from the measurement of biomass density, ρ_{Solid}, and of the bed density, ρ_{b}), X_0 ($\mathrm{kg_{extract}\ kg_{biomass}^{-1}}$) is the concentration of the target compound in the raw material, k_{f} (m h^{-1}) is the convective mass transfer coefficient around the particle (*i.e.*, broken cells), k_{s} (m h^{-1}) is the internal mass transfer coefficient in the intact cells, a (m^2 m^{-3}) is the volumetric surface area of the biomass particles, and g is the fraction of broken cells.

The BICM equations were employed to correlate the total extract removal ($w = w_{\mathrm{extract}}$) and the removal of individual target compounds/groups ($w = w_{\mathrm{i}}$). In both cases, the goodness of fit was quantified by the average absolute relative deviation (AARD) defined by:

$$\mathrm{AARD}(\%) = \frac{100}{n}\sum_{j=1}^{n}\left|\frac{\eta_{\mathrm{j}}^{\mathrm{calc}} - \eta_{\mathrm{j}}^{\mathrm{exp}}}{\eta_{\mathrm{j}}^{\mathrm{exp}}}\right| \tag{9}$$

where n is the number of points of the cumulative extraction curve, and $\eta_{\mathrm{j}}^{\mathrm{calc}}$ and $\eta_{\mathrm{j}}^{\mathrm{exp}}$ are the calculated and experimental extraction yields, respectively. The experimental results for total yield, η_{total}, and specific yield of the target compound i, η_{i}, were determined as follows:

$$\eta_{\mathrm{total}}(wt.\%) = \frac{w_{\mathrm{extract}}}{w_{\mathrm{biomass}}} \times 100 \tag{10}$$

$$\eta_{\mathrm{i}}(wt.\%) = \frac{w_i}{w_{\mathrm{biomass}}} \times 100 \tag{1}$$

The BICM input parameters are the bed porosity ε_{b}, the weight of dry biomass w_{biomass}, and the mass of extract, w_{extract} for the total extracts and w_{i} for the individual target compounds. A program coded in Matlab® (MathWorks, US) was utilized to fit the experimental data, using the Nelder-Mead simplex algorithm and setting the AARD as objective function.

Journal Pre-proof

2.7 Selectivity towards specific extractives

Selectivities were calculated for the four studied types of extractives from *V. vinifera* leaves, following the same approach of two recent SFE works [16, 21]. Selectivity was determined in terms of ratio of distributions of each group of compounds (i) over the remaining ones (non-i), in both phases: supercritical (defined by the respective extraction yields, η_{I} and $\eta_{\mathrm{non-i}}$, respectively), and the solid matrix (defined by the attainable solutes content given by $X_{0,\mathrm{I}}$ and $X_{0,\mathrm{non-i}}$, respectively). For each group, the selectivity along time ($\alpha_{\mathrm{i}}(t)$) was calculated using the following equation:

$$\alpha_{\mathrm{i}}(t) = \frac{\eta_{\mathrm{i}}(t) \times \left[X_{0,\mathrm{non-i}} - \eta_{\mathrm{non-i}}(t)\right]}{\eta_{\mathrm{non-i}}(t) \times \left[X_{0,\mathrm{i}} - \eta_{\mathrm{i}}(t)\right]} \tag{12}$$

where

$$\eta_{\mathrm{non-i}}(t) = \eta_{\mathrm{total}}(t) - \eta_{\mathrm{i}}(t) \tag{13}$$

$$X_{0,\mathrm{non-i}} = X_{0,\mathrm{total}} - X_{0,\mathrm{i}} \tag{14}$$

Here, $\eta_{\mathrm{total}}(t)$ and $\eta_{\mathrm{i}}(t)$ are the functions corresponding to the BIC model, which means $\alpha_{\mathrm{i}}(t)$ can be represented continuously along time. For clarity it is written $X_{0,\mathrm{total}}$ in Eq. (14) to emphasise that this term represents the total content of extractives, although it corresponds to our simplest notation X_0 along the article.

3 Results & Discussion

3.1 Characterization of the biomass / Soxhlet extractions

The total extraction yield (η_{total}) results ranged from 4.41 wt.% (Run Sox EA) to 16.09 wt.% (Run Sox E), as illustrated in Figure 3 (top). The polarity of the extraction solvent played a remarkably important role on the Soxhlet performance with the more polar solvent (*i.e.*, higher Hildebrand solubility parameter, δ) providing a much higher η_{total}. In detail, the amount of extract recovered by dichloromethane ($\delta = 20.2$ MPa$^{1/2}$ @ 25 ºC [50]), ethyl acetate ($\delta = 18.2$ MPa$^{1/2}$ @ 25 ºC [50]), and ethanol ($\delta = 26.2$ MPa$^{1/2}$ @ 25 ºC [50]) for the crushed leaves was 4.41, 9.18, and 16.09 wt.%, respectively. Concerning the apparent δ *vs.* η_{total} contradiction of the Soxhlet results involving EA and DCM, one should bear in mind that the extraction temperature was different in both assays, 78.4 ºC

Journal Pre-proof

for EA but just 39.6 ºC for DCM. Last but not the least, for the ground leaves the extraction yield with DCM was higher (η_{total} = 5.87 wt.%) than for the crushed leaves, emphasizing the importance of particle size reduction even for Soxhlet extraction.

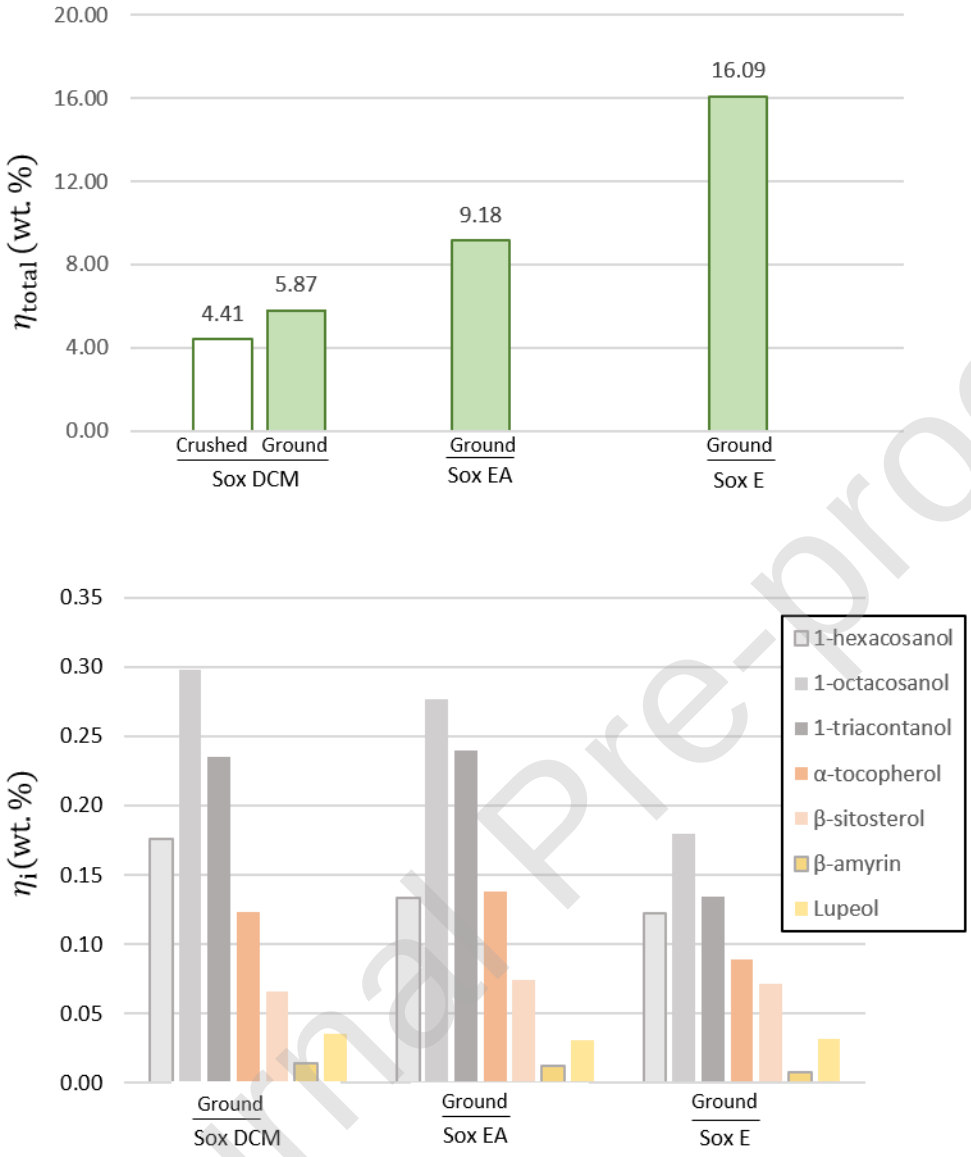

Figure 3 - Total yield (top) and individual yields (bottom) for the extracts produced from vine leaves by Soxhlet extraction with dichloromethane (DCM), ethyl acetate (EA) and ethanol (E).

Taking into account that η_{total} encompasses all the compounds that a particular solvent, extraction method and operating conditions are able to remove from the vegetal matrix, one may expect an influence of those conditions on the chemical composition of the

Journal Pre-proof

extracts. The executed GC-MS analysis allowed the identification and quantification of seven compounds, namely: 1-hexacosanol, 1-octacosanol, 1-triacontanol, α-tocopherol, *β*-sitosterol, lupeol, and *β*-amyrin. The specific yields of these compounds are presented in Figure 3 (bottom). The specific yields ranged from 0.30 wt.% for 1-octacosanol (Run Sox DCM) to 0.01 wt.% for *β*-amyrin (Run Sox E). The experimental uncertainty of the GC-MS analyses imparts an error below 0.01 % for the reported yield values.

Comparing the total (η_{total}) and individual (η_{i}) extraction yields, it is evident that the increasing η_{total} obtained for more polar solvents were not associated with higher yields of the seven target compounds. In fact, the largest η_{i} were observed for the lowest η_{total} showing that extracts from more polar solvents were enriched with other compounds (rather than the target species) having more affinity to polar media, such as carbohydrates or phenolic compounds.

For a better systematization of the work, the seven target compounds were grouped in four categories, namely: long chain aliphatic alcohols (LCAA, comprising 1-hexacosanol, 1-octacosanol, 1-triacontanol), triterpenes (*β*-amyrin and lupeol), sterols (*β*-sitosterol), and tocopherols (α-tocopherol). It is worth noting that the chemical families these groups represent are not exclusively composed by the selected molecules. However, these are the major constituents of vine leaves extracts and their investigation can shed some light on the individual performance under different extraction processes or conditions.

3.2 Supercritical fluid extraction

Total extraction yield (η_{total}) - The experimental SFE data and the BICM curves for the response η_{total} are presented in Figure 4 as function of time. Equivalent results are found when plotting the yield against the ratio of spent supercritical solvent (*i.e.*, CO_2+cosolvent) to biomass weight ($\eta_{\text{total}}\ vs.\ Q_{CO_2+\text{cosolvent}}\ t/w_{\text{biomass}}$) - please see Figure SM1 in Supplementary Material. The best performances were obtained for the combination of small particles (ground, d_{p}< 1 mm) and high amounts (10 wt.%) of cosolvent (Runs B6Ge10 and B8Gea10 – see Table 2). These conditions changed favourably the total extraction rates in comparison to pure SC-CO_2 (B4G) and to crushed particles (d_{p}< 10 mm; runs B1 to B3). In terms of final yields, after 6 h, the minimum η_{total} (1.97 wt.%) was attained for run B1 (d_{p}< 10 mm, pure SC-CO_2 and 40 ºC) and the maximum η_{total} (7.75 wt.%) was obtained in run B8Gea10 (ground particles, 10 wt.% EA and 80 ºC).

Journal Pre-proof

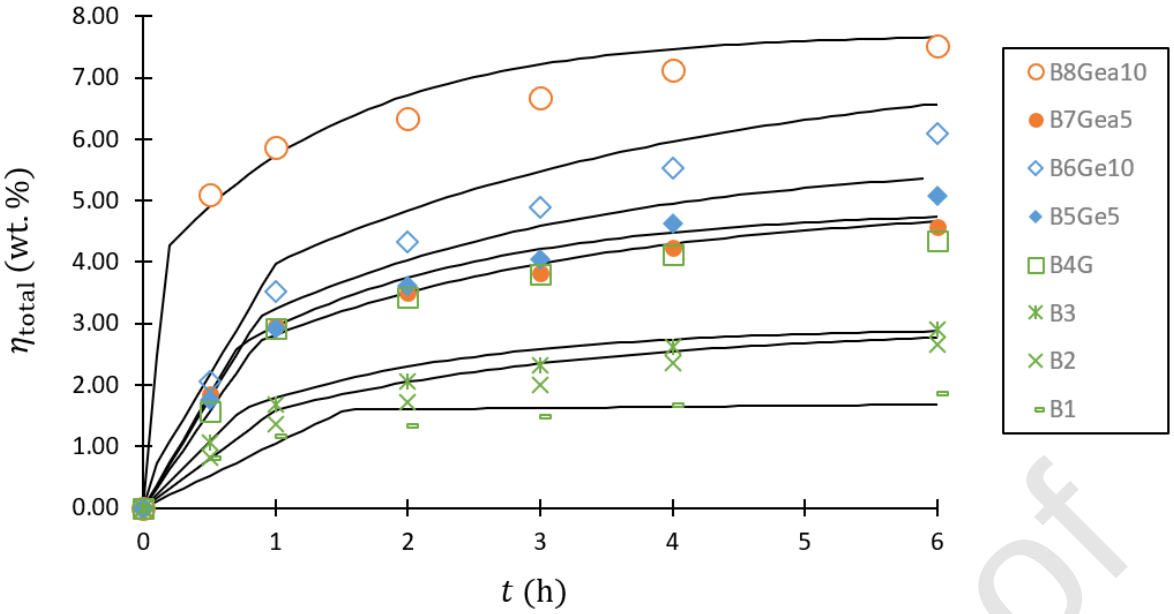

Figure 4 - Experimental data (points) and modelling results (lines; BICM). Operating conditions in Table 2.

On a comparative basis, the extractions of crushed particles (d_p< 10 mm) with pure SC-CO_2 (B1, B2, B3) failed to reach the reference η_{total} of Soxhlet with DCM (*i.e.*, 4.41 wt.%). This organic solvent is used for comparative purposes in light of the weak polar interaction that CO_2 molecule can exhibit under pressure due to its quadrupole. The total yields for these runs did not surpass 65.9 % of the reference yield, but the incremental gain imparted by temperature on the initial extraction rate is relevant: from run B1 (40 ºC) to run B3 (80 ºC), the calculated slope of η_{total} between 0.0 and 1.0 h increased from 1.2 to 1.7 wt.% h^{-1}. This extraction rate is an important parameter in any SFE process, since it determines the duration of the extraction cycle and the degree of exhaustion of the biomass, and thus the process productivity and economic viability [28,51,52]. On a different yet important line of thought, the higher temperatures also led to higher final yields, which means that as temperature increases the opposing trade-off between SC-CO_2 lower density and higher vapour pressure of compounds is favourable for the solutes extraction [53].

On the other hand, decreasing the particle size (B4G against B3) was decisive to boost η_{total}. For this run the initial extraction rate was 2.8 wt.% h^{-1} (at t = 1 h) and η_{total} was 97.7 % of the Sox DCM reference yield. However, in comparison to DCM Soxhlet

Journal Pre-proof

extraction of the ground particles (d_p< 1 mm, η_{total} = 5.8 wt.%) the final extraction yield was much smaller, reaching only 75.2 % of that value.

The better results obtained for the ground particles (Run B4G: d_p< 1 mm, ε_b = 0.81) against crushed particles (Run B3: d_p< 10 mm, ε_b = 0.94) are due to the following four reasons: (*i*) the smaller the biomass particles the higher the convective mass transfer coefficient, k_f; (*ii*) the external surface area per unit volume (a) also increases when particle size decreases; (*iii*) when porosity decreases, the interstitial velocity increases for the same mass flow rate; (*iv*) the internal resistance to mass transfer lowers when particle size decreases, although this effect is not the most important in the first period of extraction. Hence, for similar conditions and distinct particle sizes the final SFE results were 40.3 % higher for run B4G (ground particles, 80 ºC) in comparison to B3 (crushed particles, 80 ºC).

The modification of SC-CO_2 with a cosolvent was assessed at two levels of concentration (5 and 10 wt.%) for the best SFE conditions, namely ground particles (d_p< 1 mm) and 80 ºC (*i.e.*, runs B5Ge5, B6Ge10, B7Gea5, and B8Gea10). The best results were obtained for 10 wt.% of ethyl acetate (B8Gea10) with final η_{total} = 7.8 wt.% and an outstanding initial extraction rate (*ca.* 5.9 wt.% h^{-1} at t = 1 h). With 10 wt.% of ethanol (B6Ge10) the initial extraction rate was lower (*ca.* 3.5 wt.% h^{-1} at t = 1 h) and very similar to those observed without cosolvent (run B4G) and with 5 wt.% cosolvent (runs B5Ge5 and B7Gea5). Another argument is based on the Soxhlet extraction results (see Figure 3). In fact, ethyl acetate removed more extractives than DCM (9.18 wt.% *vs.* 4.41 wt.% (d_p< 10 mm) or 5.87 wt.% (d_p< 1 mm)) but significantly less than ethanol (16.1 wt.%). Overall, these observations point to a clear influence of ethyl acetate when used as cosolvent to SC-CO_2 in amounts above 5 wt.%. It should be added that ethyl acetate is used in the food industry (aroma enhancer and flavouring agent) and by the pharmaceutical industry (extraction solvent) [54] but its potential as SFE cosolvent has not been explored [28].

In general, the addition of cosolvent to SC-CO_2 improved the extraction yields especially for 10 wt.% modifications. In fact, the final (t = 6 h) yields with ethyl acetate (B8Gea10) or ethanol (B6Ge10) reached 33.5 % and 39.8 % of the respective Soxhlet yields. Concurrently, these yields were 1.7 and 1.4 times higher than the DCM Soxhlet reference yield (i.e., η_{total} = 4.4 wt.%, Figure 3*)*.

Journal Pre-proof

Extraction yield of target compounds/families (η_i) - The individual extraction curves for the grouped target compounds are presented in Figures 5 and 6. The former includes the long chain aliphatic alcohols group (LCAA: 1-hexacosanol, 1-octacosanol, 1-triacontanol) and triterpenes (β-amyrin, lupeol). The latter figure includes sterols (β-sitosterol) and tocopherols (α-tocopherol).

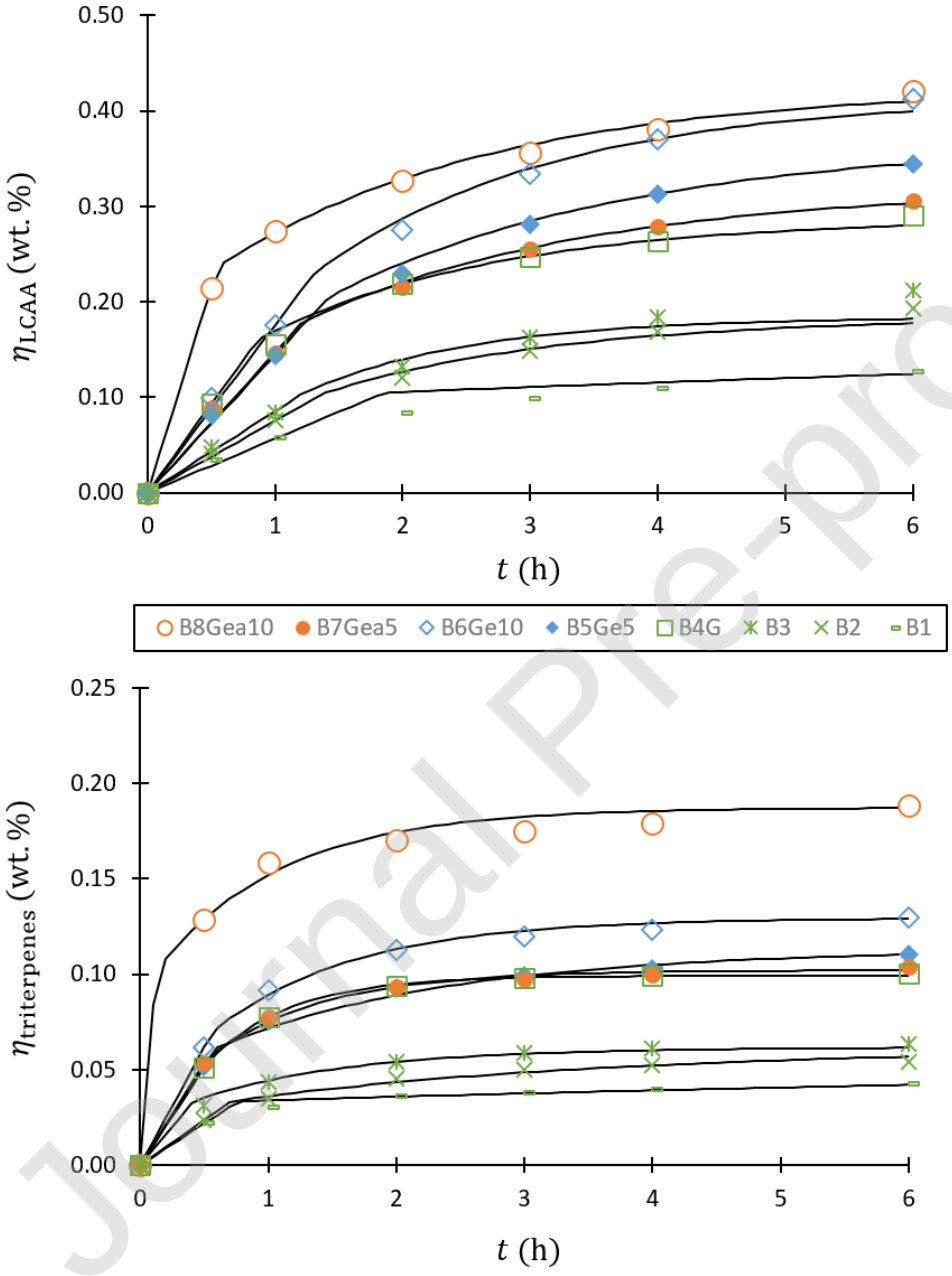

Figure 5 - Experimental data (points) and fitted BICM curves (lines) for the specific yield of LCAA (top) and triterpenes (bottom) from vine leaves. Operating conditions in Table 2.

Journal Pre-proof

The results for the LCAA group (Figure 5, top) exhibit similar trends as discussed for η_{total}. One important exception is the final yield for run B8Ge10 (η_{LCAA} = 0.41 wt.%) which converged to that of B8Gea10 (η_{LCAA} = 0.42 wt.%). These values are close to those attained by Soxhlet extraction with ethanol (0.44 wt.%) but far from the LCAA yield attained by ethyl acetate (0.65 wt.%) (see Figure 3, bottom). Hence, the total yield gain observed in run B8Ge10 cannot be related to an increased removal of the LCAA fraction. The experimental errors of the characterized alcohols were below 10 %, with an average uncertainty of ± 1 %.

The SFE results for the triterpenes group (Figure 5, bottom) appear to be congregated in three main groups: the first group (runs B1 to B3) exhibits a small initial extraction rate (*ca.* 0.043 wt.% h^{-1} at t = 1 h) and a low final yield (0.05 wt.% at t = 6 h); the second group (runs B4G, B5Ge5, B6Ge10 and B7Gea5) displays an intermediate initial extraction rate (0.08-0.09 wt.% h^{-1}) and a maximum yield in the range 0.10-0.13 wt.%; the third group (run B8Gea10) presents an high initial extraction rate (0.16 wt.% h^{-1}) and a final yield of 0.19 wt.%. Remarkably, in the latter run the $\eta_{\text{triterpenes}}$ at 0.5 h exceeded the yields of the other runs even after 6 h of operation. Moreover, the final $\eta_{\text{triterpenes}}$ attained with 10 wt.% ethyl acetate (run B8Gea10) is much higher than the specific yields for the Soxhlet runs (Figure 3). This behaviour reinforces the potential use of ethyl acetate as cosolvent for SFE of vine leaves with the goal of uptaking triterpenes. The experimental errors of the reported triterpenes SFE curves were below 13 %, with an average uncertainty of ± 3 %.

The removal of β-sitosterol (Figure 6, top) exhibits a behaviour similar to that already discussed for η_{total}, *i.e.* the initial removal rate and the final yield matched both the η_{total} trends. The final yield ranged from 0.02 wt.% (run B1) to 0.06 wt.% (run B8Gea10). The latter corresponds to 95.4 % and 85.1 % of the β-sitosterol yields obtained by Soxhlet extraction with DCM and EA, respectively. The experimental errors of the reported β-sitosterol curves stayed below 4 %, with an average uncertainty of ± 1 %.

Journal Pre-proof

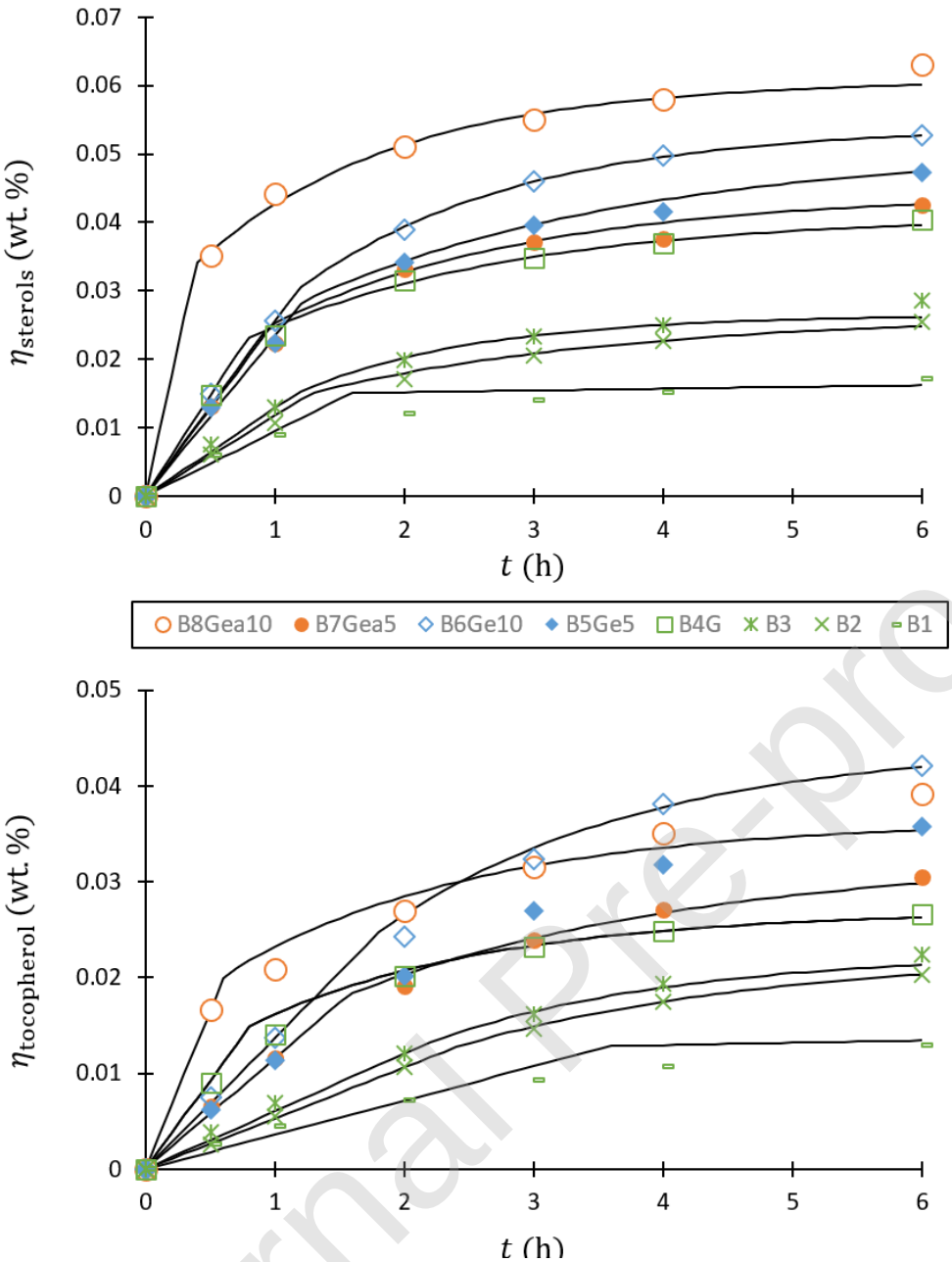

Figure 6 - Experimental data (points) and fitted BICM curves (lines) for the specific yield of sterols (top) and tocopherols (bottom) from vine leaves. Operating conditions in Table 2.

The α-tocopherol removal profiles (Figure 6, bottom) show significant differences in relation to the curves for η_{total} and for the remaining individual extractives. Firstly, α-tocopherol was the compound with the lowest SFE yields – this was not expected since $\eta_{\alpha-\text{tocopherol}}$ in the Soxhlet runs were in an intermediate position, namely above

Journal Pre-proof

$\eta_{\beta-\text{sitosterol}}$ and η_{i} for the individual triterpenes (β-amyrin and lupeol). Secondly, the extraction yield for 10 wt.% ethyl acetate (run B8Gea10) was higher only up to 2 h of operation and then it was surpassed by the yield curve for 10 wt.% ethanol (run B6Ge10). The highest result, $\eta_{\alpha-\text{tocopherol}} = 0.04$ wt. %, represents only 32.5 % and 29.0 % of the Soxhlet extraction yields with DCM and EA, respectively. The experimental errors of the reported α-tocopherol curves remained below 5 %, with an average uncertainty of ± 1 %.

3.3 Phenomenological modeling

The broken plus intact cells model (BICM) was simultaneously fitted to all SFE data of the five different responses (η_{total} and the individual extraction yields of η_{LCAA}, $\eta_{\text{triterpenes}}$, $\eta_{\beta-\text{sitosterol}}$ and $\eta_{\alpha-\text{tocopherol}}$), which means that 40 curves were modelled. The rationale was adapted from a previous modelling study focussing on SFE of cork [42] and is explained in the following lines.

The BICM fitting parameters were $g, X_0, y^*, k_{\text{f}}a$, and $\text{k}_{\text{s}}a$. The fraction of broken cells (g) was a shared parameter for the assays with identical particle sizes thus being different for crushed or ground leaves. The extract concentration in the raw material (X_0) was common only for runs using the same particle size and the same SCF composition. By doing so mass balance changes can be accommodated whenever biomass structure is modified or the molecular nature of the supercritical solvent (pure or mixture) is tuned. Solubility (y^*) was only shared for runs B3 and B4G, because of equal and $P-T$ conditions and SCF composition. The mass transfer parameters, $k_{\text{f}}a$ and $\text{k}_{\text{s}}a$, were fitted individually as they are expected to change with temperature, particle size, and SCF composition.

Total extraction yield (η_{total}) - The fitting of BICM to the eight extraction curves led to good quality results translated by AARD values ranging from 1.05 to 12.54 %, or 4.06 % globally, as shown in Table 3. The adjusted kinetic curves are presented (lines) in Figure 4 and the optimized parameters for the total yield responses, including the CER and FER times, are listed in Table 3.

The calculated fraction of broken cells was slightly higher for the ground particles (g = 0.442) than for the crushed particles (g = 0.432), which was expected in advance. For the assays with pure SC-CO_2 and crushed leaves (runs B1, B2, B3), for fixed amount of attainable extractives (X_0 = 0.029 kg kg^{-1}) one can observe an increase of solubility (y^*) and intraparticle diffusion ($k_{\text{s}}a$) with increasing temperature. For the film coefficient, $k_{\text{f}}a$,

Journal Pre-proof

the influence of temperature is notorious since the value for run B1 (40 ºC) is the lowest (0.055 h^{-1}) and those of B3 (80 ºC) is the highest (0.071 h^{-1}). Hence, the fitting results fully support the decision to operate at high temperature (80 ºC) because the mass transfer parameters are enhanced.

Table 3 - BICM fitting results for the total extraction yield.

Run	Fitted parameters					Calculated parameters		AARD (%)
	$k_f a$ (h^{-1})	$k_s a$ (h^{-1})	γ^*	X_0 (kg kg^{-1})	g	t_{CER}	t_{FER} (h)	
B1	0.055	0.001	0.017	0.029	0.432	1.59	1.60	12.54
B2	0.066	0.023	0.024	"	"	1.04	1.06	4.67
B3	0.071	0.032	0.034	"	"	0.76	0.78	3.79
B4G	0.371	0.075	"	0.050	0.442	0.87	0.90	3.17
B5Ge5	0.766	0.075	0.018	0.057	"	0.88	0.92	2.61
B6Ge10	0.437	0.057	0.033	0.074	"	1.12	1.15	3.34
B7Gea5	0.304	0.103	0.047	0.049	"	0.73	0.74	1.05
B8Gea10	0.924	0.133	0.105	0.077	"	0.17	0.18	1.34
Total								**4.06**

Significant differences were observed for $k_f a$ in runs B3 and B4G, both performed with pure SC-CO_2 at 80 ºC differing only in the particle size. For the ground particles (run B4G) $k_f a$ was more than five times higher than for crushed particles (run B3). This behaviour might be explained not only by the higher specific surface area (a) of the ground leaves but also by the lower bed porosity (ε_b = 0.81 for B4G against ε_b = 0.94 for B1) that gives rise to higher interstitial velocity of the percolating solvent. Modelling results clearly indicate that grinding the leaves enhances the kinetic performance of SFE.

In terms of the impact of cosolvent, one must distinguish the first hour of extraction (nearly the CER period) from the remaining period: (*i*) in the first hour, the addition of 10 wt.% ethyl acetate has an outstanding impact on η_{total} as the values of $k_f a$ and γ^* in Table 3 corroborate. This effect is even higher than in the case of 10 wt.% ethanol. (*ii*) after one hour, all yield curves continuously increase but at different rates. While in the case of ethyl acetate a slower pace is observed, for ethanol an almost linear increase of the yield is observed. The modeling results shown in Figure 4 are in accordance with the experimental trends. (*iii*) Notwithstanding the previous finding may suggest a convergence to the

Journal Pre-proof

Soxhlet yields (where ethanol reaches a much higher value than ethyl acetate), it is worth noting that the pure solvents (CO_2, E, EA) and the modified supercritical fluids (CO_2 + 5 % E, CO_2 + 10 % E, CO_2 + 5 % EA, CO_2 + 10 % EA) are distinct solvents with different absolute extraction capacities and kinetics.

Analysing the duration of the BICM characteristic extraction periods, t_{CER} and t_{FER}, one may note small differences within each assay and a strong influence of the operating conditions. In particular, t_{CER} ranged from 0.17 h (run B8Gea10) to 1.59 h (run B1) becoming smaller for higher temperatures 1.59 h at 40 ºC (run B1) and 0.76 h at 80 ºC (run B3). The addition of ethanol (5 or 10 wt.%) did not shorten the CER period (t_{CER} *ca.* 0.9-1.1 h, in runs B5Ge5 and B6Ge10). However, the CO_2 modified with ethyl acetate lowered the CER period especially with the addition of 10 wt.% (t_{CER} is 0.73 h with 5 wt.% EA and 0.17 h with 10 wt.% EA).

All in all, for the SFE curves modelled with BICM, the ratios of $k_{\mathrm{f}}a/k_{\mathrm{s}}a$ worth from 2 to 55, corroborating that the SFE of vine leaves is limited by intraparticle diffusion. Apparently, the diffusion-controlled (DC) period initiates after 0.18–1.60 h and the X_0 values are only attained after entering in the DC period.

Extraction yield of target compounds/families (η_{i}) - Regarding the target compounds / families of compounds, emphasis will be given to the performance and trends that deviate from those discussed for η_{total}. The BICM fitting results for LCAA yields are presented in Table 4. The AARD values are in the range 1.30-6.00 %, except for run B1 (10.81 %) as previously observed for η_{total}. In terms of trends, solubility (γ^*) decreased with increasing amounts of ethanol (E), going from 0.0019 without E (run B4G) to 0.0015 and then 0.0012 with 5 and 10 wt.% E, respectively (runs B5Ge5 and B6Ge10). Another noteworthy behaviour is a general delay of the LCAA specific t_{CER} and t_{FER} indicators, with an offset (up to 0.5 h) for the diffusion-controlled (DC) period for this group in relation to the total extracts.

Table 4 - BICM fitting results for the extraction yield of long chain aliphatic alcohols (LCAA).

Run	Fitted parameters					Calculated parameters		AARD (%)
	$k_{\mathrm{f}}a$ (h^{-1})	$k_{\mathrm{s}}a$ (h^{-1})	γ^*	X_0 (kg kg^{-1})	g	t_{CER}	t_{FER} (h)	

Journal Pre-proof

B1	0.0372	0.0038	0.0013	0.0018	0.432	1.85	1.86	10.81
B2	0.0442	0.0295	0.0016	"	"	1.38	1.40	4.23
B3	0.0479	0.0416	0.0019	"	"	1.22	1.23	6.00
B4G	0.3686	0.1045	"	0.0029	0.442	0.85	0.88	2.26
B5Ge5	0.3566	0.0817	0.0015	0.0037	"	1.41	1.45	3.02
B6Ge10	0.5467	0.1033	0.0012	0.0041	"	1.30	1.35	3.47
B7Gea5	0.2801	0.0873	0.0019	0.0032	"	1.20	1.23	3.45
B8Gea10	0.6112	0.0894	0.0025	0.0043	"	0.54	0.56	1.30
Total								**4.32**

The BICM results for $\eta_{\text{triterpenes}}$ are displayed in Table 5. Particularly low errors were obtained, even for run B1, in the range 0.46 to 3.29 %. The $k_f a$ and X_0 values are grouped in a way that resembles the grouping used to discuss the SFE curve performances. This emphasises the favourable reduction of particle size and the CO_2 modification with 10 wt.% EA. Lastly, the trends on the characteristic extraction periods were distinct even in comparison to LCAA. In fact, t_{CER} and t_{FER} for triterpenes are generally lower (0.2-0.8 h) than for η_{total}, with the exception of Run B8Gea10. As a result, the specific uptake of triterpenes reached faster the DC period than the bulk extract.

Table 5 - BICM fitting results for the extraction yield of triterpenes.

Run	Fitted parameters					Calculated parameters		AARD (%)
	$\boldsymbol{k_f a}$ (h^{-1})	$\boldsymbol{k_s a}$ (h^{-1})	$\boldsymbol{\gamma^*}$	$\boldsymbol{X_0}$ (kg kg^{-1})	$\boldsymbol{g}$	$\boldsymbol{t_{CER}}$	$\boldsymbol{t_{FER}}$ (h)	
B1	0.0284	0.0038	0.0013	0.00062	0.432	0.77	0.77	2.21
B2	0.0338	0.0183	0.0013	"	"	0.71	0.72	2.67
B3	0.0367	0.0452	0.0024	"	"	0.42	0.42	3.29
B4G	0.1632	0.3014	"	0.00099	0.442	0.53	0.53	0.46
B5Ge5	0.3151	0.1063	0.0012	0.0011	"	0.59	0.60	1.97
B6Ge10	0.3862	0.1745	0.0012	0.0013	"	0.56	0.58	1.36
B7Gea5	0.2388	0.2188	0.0016	0.0010	"	0.51	0.52	1.37
B8Gea10	0.6933	0.1946	0.0044	0.0019	"	0.12	0.12	2.54
Total								**1.98**

The AARD values for the $\eta_{\beta-\text{sitosterol}}$ curves stayed within 1.73 and 4.03 % except for run B1, as reported in Table 6. The resemblance of the parameter trends with those of η_{total} was substantial for this response. This was also observed for the duration of the CER and FER periods, which remained close to those of the total yield (average differences < 0.1 h).

Journal Pre-proof

Table 6 - BICM fitting results for the extraction yield of β-sitosterol.

Run	Fitted parameters					Calculated parameter		AARD (%)
	$\boldsymbol{k_f a}$ (h^{-1})	$\boldsymbol{k_s a}$ (h^{-1})	$\boldsymbol{\gamma^*}$	$\boldsymbol{X_0}$ (kg kg^{-1})	$\boldsymbol{g}$	$\boldsymbol{t_{CER}}$	$\boldsymbol{t_{FER}}$ (h)	
B1	0.0420	0.0013	0.00020	0.00026	0.432	1.58	1.59	12.36
B2	0.0500	0.0225	0.00023	"	"	1.27	1.28	3.84
B3	0.0542	0.0398	0.00026	"	"	1.16	1.17	4.03
B4G	0.4399	0.0951	"	0.00041	0.442	0.76	0.78	1.73
B5Ge5	0.2657	0.0741	0.00032	0.00051	"	1.21	1.23	3.30
B6Ge10	0.2460	0.1142	0.00038	0.00054	"	1.17	1.19	2.73
B7Gea5	0.1632	0.0959	0.00058	0.00044	"	0.93	0.94	3.61
B8Gea10	1.0479	0.1261	0.00030	0.00061	"	0.38	0.40	2.02
Total								**4.20**

Finally, the errors for $\eta_{\alpha-\text{tocopherol}}$ curves were between 1.31 and 7.17 %, except for run B1 that reached 14.92 % (see Table 7). The main differences between runs were observed for crushed and ground particles, especially for the film mass transfer coefficients (one order of magnitude higher for the small particles). The influence of cosolvents was noticed in distinct ways: while EA led mainly to a solubility enhancement, the use of E translated into a film diffusion gain. This explains the overlapping of B6Ge10 and B8Gea10 curves seen in Figure 6.

By setting a crossed comparison between the adjusted parameters ruling the extraction kinetics ($k_f a$, and $k_s a$) for both the different chemical families and the whole extract (as a pseudo-component), interesting conclusions can be drawn. In terms of convective film diffusion ($k_f a$), the four target families exhibit average (*i.e.* the 8 runs) convective coefficients that amount only 42 to 68 % of those of the whole extract, with LCCA and β-sitosterol sharing the highest value, tocopherol the lowest, and triterpenes right in between (55 %). This reveals a worse performance of these families in comparison to other bulk compounds that were co-removed. A different picture arises from the analysis of the fitted average intraparticle diffusion parameters ($k_s a$). Here, triterpenes outcast with average parameter amounting two times those of the rest of the families (which scored all identically), as well as those of the whole extract (i.e., including all compounds that were extracted). This suggests a favourable appetence for the uptake of the triterpenes family from inner positions of biomass particles, which is decisive when the whole phenomenon relies preferably on this type of diffusion resistance to mass transfer.

Journal Pre-proof

Table 7 - BICM fitting results for the extraction yield of α-tocopherol.

Run	Fitted parameters					Calculated parameters		AARD (%)
	$\boldsymbol{k_f a}$ (h^{-1})	$\boldsymbol{k_s a}$ (h^{-1})	$\boldsymbol{\gamma}^*$	$\boldsymbol{X_0}$ (kg kg^{-1})	$\boldsymbol{g}$	$\boldsymbol{t_{CER}}$	$\boldsymbol{t_{FER}}$ (h)	
B1	0.0171	0.0014	0.00018	0.00022	0.432	3.58	3.59	14.92
B2	0.0204	0.0225	0.00025	"	"	2.42	2.43	1.31
B3	0.0221	0.0291	0.00029	"	"	2.12	2.13	7.17
B4G	0.2389	0.1048	"	0.00027	0.442	0.81	0.82	3.84
B5Ge5	0.3379	0.0839	0.00012	0.00039	"	1.89	1.93	4.03
B6Ge10	0.3963	0.0960	0.00013	0.00044	"	1.78	1.83	3.84
B7Gea5	0.1016	0.0713	0.00042	0.00033	"	1.56	1.57	3.61
B8Gea10	0.2680	0.0986	0.00044	0.00036	"	0.61	0.62	5.19
Total								**5.49**

3.4 Selectivity towards specific extractives

The cumulative selectivity curves are presented in Figure 7 for LCAA (top left), triterpenes (top right), β − sitosterol (bottom left), an α − tocopherol d (bottom right). For an easier appraisal, $\alpha_i\,(t)$ is provided for selected runs that evidence the impact of biomass particle size and SCF composition, namely B3, B4G, B6Ge10, and B8Gea10.

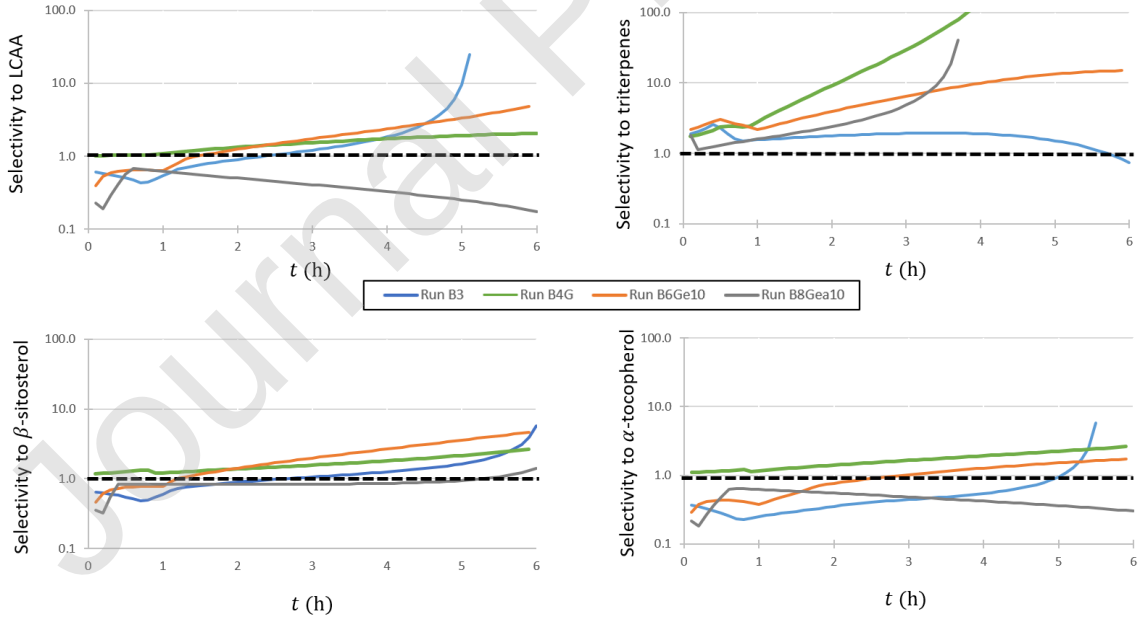

Figure 7 - Selectivity towards target compounds/families of extractives calculated for the cumulative extracts of the SFE curves.

Journal Pre-proof

Starting with LCAA, the results show that in the first hours of the SFE experiments selectivity to LCAA was unfavorable ($\alpha_{\mathrm{LCAA}} < 1$) and afterwards two behaviours can be seen: a slow pace correction towards $\alpha_{\mathrm{LCAA}} > 1$ for the runs without cosolvent (B3, B4G) or with ethanol (B6Ge10); and a stronger decrease of selectivity towards LCAA ($\alpha_{\mathrm{LCAA}} \ll 1$) along time in the case of EA addition (B8Gea10).

A rather distinct performance was found for triterpenes. For this group, the SFE runs initiated under a clearly selective uptake ($1.7 < \alpha_{\mathrm{triterpenes}} < 2.2$) and increased along time reaching values above 10 for SFE extraction with ground particles with pure or modified CO_2. A distinct behaviour is noticeable when processing crushed particles (run B3) with $\alpha_{\mathrm{triterpenes}}$ maintaining a score around 1.9 for most of the time and then decreasing to less than 1 in the last two hours of extraction.

The selectivity trends towards $\beta-\mathrm{sitosterol}$ resemble those for LCAA, excluding the negative influence of ethyl acetate on the competitive removal of the latter. Consequently, the $\alpha_{\mathrm{i}}\,(t)$ profiles start in the vicinity of $\alpha_{\beta-\mathrm{sitosterol}} \sim 1$ and evolve favourably to values from 1.4 to 5.8. As far as $\alpha-\mathrm{tocopherol}$ is concerned, an unfavorable selectivity ($\alpha_{\alpha-\mathrm{tocopherol}} < 1$) was explicit during the first half of extraction for all assays excepting run B4G. The latter increased at constant pace from $\alpha_{\alpha-\mathrm{tocopherol}} \sim 1$ to a final score of 2.6. Therefore, the selectivity to this compound is more influenced by particle size than by SCF composition.

An important observation allowed by the results of Figure 7 is that the selection and use of a cosolvent to tune the affinity of CO_2 towards target compounds (argument many times invoked in SFE works) is not necessarily beneficial for the selectivity enhacement despite the apparent gain of yields along time (*i.e.*, productivity). Accordingly, under the same particle size conditions (i.e, excluding run B3) in none of the cases did the addition of ethanol or ethyl acetate lead to an initial undisputable gain of selectivity in relation pure CO_2. However, target families like LCCA, $\beta-\mathrm{sitosterol}$ and α-tocopherol, lowered the selectivity in spite of using cosolvents of an intermediate (ethyl acetate) or more pronounced (ethanol) polarity. In turn, for triterpenes ethanol provided a similar selectivity of pure CO_2 during the first hour of uptake but was then relegated to a worse performance. As a result, the results attained in this work emphasize the need for a balance between productivity and selectivity when opting for the inclusion of cosolvent, with a chance that decision is much more relevant for productivity enhancement than selectivity gains.

Journal Pre-proof

Overall, the selectivity demonstrates that both particle size and cosolvent addition play a non-negligible role in the competitive removal of the different types of extractives. In particular, upon attaining selectivity profiles scoring above 1 since the onset and evolving to values between 10 and 100, the outstanding capacity of SC-CO_2 (either pure or modified) to extract triterpenes lupeol and *β*-amyrin from the leaves of *V. vinifera* was verified.

4. Conclusions

The supercritical fluid extraction (SFE) of grape leaves (*Vitis vinifera L.*) was investigated for the first time. GC-MS characterization of the extracts allowed the identification and quantification of long chain aliphatic alcohols (LCAA; namely, 1-hexacosanol, 1-octacosanol and 1-triacontanol) plus interesting bioactive compounds such as *α*-tocopherol, *β*-sitosterol and the triterpenes *β*-amyrin and lupeol.

The SFE experiments were performed using crushed (< 10 mm) and ground (< 1 mm) biomass, and the total yield ranged from 1.86 to 7.52 wt.% with the best results corresponding to the extraction of ground particles using SC-CO_2 with 10 wt.% ethyl acetate, at 80 ºC. The individual yields of target molecules were much smaller, ranging from 0.13 to 0.42 wt.% for LCAA, 0.04 to 0.19 wt.% for triterpenes, 0.02 to 0.06 wt.% for *β*-sitosterol, and 0.01 to 0.04 wt.% for *α*-tocopherol. The SFE kinetic curves were fitted using the broken plus intact cells model (BICM), and the modelling results indicated that the extraction of vine leaves is limited by intraparticle diffusion.

At selectivity level, remarkable results were attained for triterpenes (lupeol and β-amyrin), starting at 1.7 and increasing along time to values between 10 and 100. Both particle size and cosolvent addition played a significant role on the selective removal of target compounds from the biomass. The reported results highlight the pertinence of determining the target compounds selectivity in SFE works, and demonstrate that SC-CO_2 has a tuneable affinity to the different lipophilic compounds present in *V. vinifera* L. leaves.

Declaration of interests

The authors declare that they have no known competing financial interests or personal relationships that could have appeared to influence the work reported in this paper.

Journal Pre-proof

5. Acknowledgement

This work was developed within the scope of the project CICECO-Aveiro Institute of Materials, UIDB/50011/2020 & UIDP/50011/2020, financed by national funds through the FCT/MEC and when appropriate co-financed by FEDER under the PT2020 Partnership Agreement. Authors want to thank the funding from Project AgroForWealth (CENTRO-01-0145-FEDER-000001), funded by Centro2020, through FEDER and PT2020.

6. References

[1] Wines of Portugal, Wines of Portugal: Production, http://www.winesofportugal.info (accessed February 2019).

[2] A. Teixeira, N. Baenas, R. Dominguez-Perles, A. Barros, E. Rosa, D. Moreno, C. Garcia-Viguera, Natural Bioactive Compounds from Winery By-Products as Health Promoters: A Review, International Journal of Molecular Sciences 15 (2014) 15638–15678.

[3] F. Fernandes, E. Ramalhosa, P. Pires, J. Verdial, P. Valentão, P. Andrade, A. Bento, J.A. Pereira, *Vitis vinifera* leaves towards bioactivity, Industrial Crops and Products. 43 (2013) 434–440.

[4] F. Pensec, A. Szakiel, C. Pączkowski, A. Woźniak, M. Grabarczyk, C. Bertsch, M.J.C. Fischer, J. Chong, Characterization of triterpenoid profiles and triterpene synthase expression in the leaves of eight *Vitis vinifera* cultivars grown in the Upper Rhine Valley, Journal of Plant Research 129 (2016) 499–512.

[5] (-)-alpha-Tocopherol | C29H50O2 - PubChem, https://pubchem.ncbi.nlm.nih.gov/compound/alpha-Tocopherol (accessed February 2019).

[6] C. Yang, Z.Y. Chen, S.L. Wong, J. Liu, Y.T. Liang, C.W. Lau, H.K. Lee, Y. Huang, S.Y. Tsang, β-Sitosterol oxidation products attenuate vasorelaxation by increasing reactive oxygen species and cyclooxygenase-2, Cardiovascular Research 97 (2013)

Journal Pre-proof

520–532.

[7] P.K. Chaturvedi, K. Bhui, Y. Shukla, Lupeol: Connotations for chemoprevention, Cancer Letters. 263 (2008) 1–13.

[8] K.A.B. Simão da Silva, A.F. Paszcuk, G.F. Passos, E.S. Silva, A.F. Bento, F.C. Meotti, J.B. Calixto, Activation of cannabinoid receptors by the pentacyclic triterpene *α,β*-amyrin inhibits inflammatory and neuropathic persistent pain in mice, Pain 152 (2011) 1872–1887.

[9] X. Yao, G. Li, Q. Bai, H. Xu, C. Lü, Taraxerol inhibits LPS-induced inflammatory responses through suppression of TAK1 and Akt activation, International Immunopharmacology 15 (2013) 316–324..

[10] M.M.R. de Melo, I. Portugal, A.J.D. Silvestre, C.M. Silva, Environmentally benign supercritical fluid extraction, in: M.T. Francisco Pena-Pereira (Ed.), The Application of Green Solvents in Separation Processes, Elsevier, 2017.

[11] L. Baldino, E. Reverchon, Challenges in the production of pharmaceutical and food related compounds by SC-CO2 processing of vegetable matter, Journal of Supercritical Fluids. 134 (2018) 269–273.

[12] M. Marchi, E. Neri, F.M. Pulselli, S. Bastianoni, CO_2 recovery from wine production: Possible implications on the carbon balance at territorial level, Journal of CO2 Utilization. 28 (2018) 137–144.

[13] F. Bashipour, S.M. Ghoreishi, Response surface optimization of supercritical CO_2 extraction of α-tocopherol from gel and skin of *Aloe vera* and almond leaves, Journal of Supercritical Fluids 95 (2014) 348–354.

[14] Q. Hu, Y. Hu, J. Xu, Free radical-scavenging activity of *Aloe vera* (*Aloe barbadensis* Miller) extracts by supercritical carbon dioxide extraction, Food Chemistry 91 (2005) 85–90.

[15] P.G. Vieira, M.M.R. de Melo, A. Şen, M.M.Q. Simões, I. Portugal, H. Pereira, C.M. Silva, *Quercus cerris* extracts obtained by distinct separation methods and solvents: total and friedelin extraction yields, and chemical similarity analysis by

Journal Pre-proof

multidimensional scaling, Separation and Purification Technology (2019) 115924.

[16] M.M.R. de Melo, A. Şen, A.J.D. Silvestre, H. Pereira, C.M. Silva, Experimental and modeling study of supercritical CO 2 extraction of *Quercus cerris* cork: Influence of ethanol and particle size on extraction kinetics and selectivity to friedelin, Separation and Purification Technology 187 (2017) 34-45.

[17] V.H. Rodrigues, M.M.R. de Melo, I. Portugal, C.M. Silva, Supercritical fluid extraction of *Eucalyptus globulus* leaves. Experimental and modelling studies of the influence of operating conditions and biomass pretreatment upon yields and kinetics, Separation and Purification Technology 191 (2018) 173-181.

[18] V.H. Rodrigues, M.M.R. de Melo, I. Portugal, C.M. Silva, Extraction of *Eucalyptus leaves* using solvents of distinct polarity. Cluster analysis and extracts characterization, Journal of Supercritical Fluids 135 (2018) 263–274.

[19] C. Da Porto, D. Voinovich, D. Decorti, A. Natolino, Response surface optimization of hemp seed (*Cannabis sativa* L.) oil yield and oxidation stability by supercritical carbon dioxide extraction, Journal of Supercritical Fluids 68 (2012) 45–51.

[20] A.C. Gallo-Molina, H.I. Castro-Vargas, W.F. Garzón-Méndez, J.A. Martínez Ramírez, Z.J. Rivera Monroy, J.W. King, F. Parada-Alfonso, Extraction, isolation and purification of tetrahydrocannabinol from the *Cannabis sativa* L. plant using supercritical fluid extraction and solid phase extraction, The Journal of Supercritical Fluids 146 (2019) 208–216.

[21] M.M.R. de Melo, R.P. Silva, A.J.D. Silvestre, C.M. Silva, Valorization of water hyacinth through supercritical CO_2 extraction of stigmasterol, Industrial Crops and Products 80 (2016) 177-185.

[22] M.M.R. De Melo, P.F. Martins, A.J.D. Silvestre, P. Sarmento, C.M. Silva, Measurement and modeling of supercritical fluid extraction curves of *Eichhornia crassipes* for enhanced stigmasterol production: Mechanistic insights of the process, Separation and Purification Technology 163 (2016) 189-198.

[23] J. Ortiz-Viedma, N. Romero, L. Puente, K. Burgos, M. Toro, L. Ramirez, A. Rodriguez, J. Barros-Velazquez, S.P. Aubourg, Antioxidant and antimicrobial

Journal Pre-proof

effects of stevia (*Stevia rebaudiana* Bert.) extracts during preservation of refrigerated salmon paste, European Journal of Lipid Science and Technology 119 (2017) 1600467.

[24] K. Ameer, B.-S. Chun, J.-H. Kwon, Optimization of supercritical fluid extraction of steviol glycosides and total phenolic content from *Stevia rebaudiana* (Bertoni) leaves using response surface methodology and artificial neural network modeling, Industrial Crops and Products 109 (2017) 672–685.

[25] M.M.R. de Melo, R.M.A. Domingues, A.J.D. Silvestre, C.M. Silva, Extraction and purification of triterpenoids using supercritical fluids: from lab to exploitation, Mini-Reviews in Organic Chemistry 11 (2014) 362-381.

[26] S. Zhao, D. Zhang, Supercritical fluid extraction and characterisation of *Moringa* oleifera leaves oil, Separation and Purification Technology 118 (2013) 497-502.

[27] A. Rai, B. Mohanty, R. Bhargava, Modeling and response surface analysis of supercritical extraction of watermelon seed oil using carbon dioxide, Separation and Purification Technology 141 (2015) 354–365.

[28] M.M.R. De Melo, A.J.D. Silvestre, C.M. Silva, Supercritical fluid extraction of vegetable matrices: Applications, trends and future perspectives of a convincing green technology, Journal of Supercritical Fluids. 92 (2014) 115-176.

[29] R.M.A. Domingues, E.L.G. Oliveira, C.S.R. Freire, R.M. Couto, P.C. Simões, C.P. Neto, A.J.D. Silvestre, C.M. Silva, Supercritical Fluid Extraction of *Eucalyptus globulus* Bark—A Promising Approach for Triterpenoid Production, International Journal of Molecular Sciences. 13 (2012) 7648–7662.

[30] S. Li, S. Hartland, Influence of co-solvents on solubility and selectivity in extraction of xanthines and cocoa butter from cocoa beans with supercritical CO_2, Journal of Supercritical Fluids. 5 (1992) 7–12.

[31] C.P. Passos, R.M. Silva, F.A. Da Silva, M.A. Coimbra, C.M. Silva, Supercritical fluid extraction of grape seed (*Vitis vinifera* L.) oil. Effect of the operating conditions upon oil composition and antioxidant capacity, Chemical Engineering Journal. 160 (2010) 634-640.

Journal Pre-proof

[32] K.S. Duba, L. Fiori, Supercritical CO_2 extraction of grape seed oil: Effect of process parameters on the extraction kinetics, Journal of Supercritical Fluids. 98 (2015) 33–43.

[33] L. Fiori, Grape seed oil supercritical extraction kinetic and solubility data: Critical approach and modeling, Journal of Supercritical Fluids. 43 (2007) 43–54.

[34] C.P. Passos, R.M. Silva, F.A. Da Silva, M.A. Coimbra, C.M. Silva, Enhancement of the supercritical fluid extraction of grape seed oil by using enzymatically pre-treated seed, Journal of Supercritical Fluids. 48 (2009) 225–229.

[35] L. Fiori, Supercritical extraction of grape seed oil at industrial-scale: Plant and process design, modeling, economic feasibility, Chemical Engineering and Processing: Process Intensification. 49 (2010) 866–872.

[36] C. Da Porto, A. Natolino, Supercritical fluid extraction of polyphenols from grape seed (V*itis vinifera*): Study on process variables and kinetics, Journal of Supercritical Fluids. 130 (2017) 239–245.

[37] V. V. Cotea, C. Luchian, M. Niculaua, C.I. Zamfir, I. Moraru, B.C. Nechita, C. Colibaba, Evaluation of phenolic compounds content in grape seeds, Environmental Engineering and Management Journal. 17 (2018) 795–803.

[38] T.H.J. Beveridge, B. Girard, T. Kopp, J.C.G. Drover, Yield and Composition of Grape Seed Oils Extracted by Supercritical Carbon Dioxide and Petroleum Ether: Varietal Effects, Journal of Agricultural and Food Chemistry. 53 (2005) 1799–1804.

[39] C.S.R. Freire, A.J.D. Silvestre, C.C.L. Pereira, C.P. Neto, J.A.S. Cavaleiro, New lipophilic components of pitch deposits from an *Eucalyptus globulus* ECF bleached kraft pulp mill, Journal of Wood Chemistry and Technology. 22 (2002) 55–66.

[40] ChemSpider, http://www.chemspider.com/ (accessed February 2019).

[41] R.M.A. Domingues, M.M.R. de Melo, E.L.G. Oliveira, C.P. Neto, A.J.D. Silvestre, C.M. Silva, Optimization of the supercritical fluid extraction of triterpenic acids from *Eucalyptus globulus* bark using experimental design, Journal of Supercritical Fluids. 74 (2013) 105–114.

Journal Pre-proof

[42] M.M.R. de Melo, A. Şen, A.J.D. Silvestre, H. Pereira, C.M. Silva, Experimental and modeling study of supercritical CO_2 extraction of *Quercus cerris* cork: Influence of ethanol and particle size on extraction kinetics and selectivity to friedelin, Separation and Purification Technology 187 (2017) 34-45.

[43] K.S. Pitzer, D.R. Schreiber, Improving equation-of-state accuracy in the critical region - equations for carbon-dioxide and neopentane as examples, Fluid Phase Equilibria. 41 (1988) 1–17.

[44] H. Pöhler, E. Kiran, Volumetric Properties of Carbon Dioxide + Ethanol at High Pressures, 42:2 (1997) 384-388.

[45] M. Kato, D. Kodama, T. Ono, M. Kokubo, Volumetric Properties of Carbon Dioxide + Ethanol at 313.15 K, Journal of Chemical & Engineering Data. 54 (2009) 2953–2956.

[46] N. Falco, E. Kiran, Volumetric properties of ethyl acetate + carbon dioxide binary fluid mixtures at high pressures, The Journal of Supercritical Fluids. 61 (2012) 9–24.

[47] C.S.R. Freire, A.J.D. Silvestre, C.P. Neto, J.A.S. Cavaleiro, Lipophilic Extractives of the Inner and Outer Barks of *Eucalyptus globulus*, Holzforschung. 56 (2002) 372–379.

[48] H. Sovová, R.P. Stateva, Supercritical fluid extraction from vegetable materials, Reviews in Chemical Engineering 27 (2011) 79–156.

[49] H. Sovová, Mathematical model for supercritical fluid extraction of natural products and extraction curve evaluation, Journal of Supercritical Fluids. 33 (2005) 35–52.

[50] A.F.M. Barton, CRC handbook of solubility parameters and other cohesion parameters, CRC Press, 1991.

[51] N.C.M.C.S. Leitão, G.H.C. Prado, P.C. Veggi, M.A.A. Meireles, C.G. Pereira, *Anacardium occidentale* L. leaves extraction via SFE: Global yields, extraction kinetics, mathematical modeling and economic evaluation, Journal of Supercritical Fluids. 78 (2013) 114–123.

[52] M.M.R. De Melo, H.M.A. Barbosa, C.P. Passos, C.M. Silva, Supercritical fluid

Journal Pre-proof

extraction of spent coffee grounds: Measurement of extraction curves, oil characterization and economic analysis, Journal of Supercritical Fluids. 86 (2014) 150-159.

[53] M.M.R. De Melo, E.L.G. Oliveira, A.J.D. Silvestre, C.M. Silva, Supercritical fluid extraction of triterpenic acids from *Eucalyptus globulus* bark, Journal of Supercritical Fluids. 70 (2012).

[54] SEKAB, Ethyl acetate - An Organic Solvent, http://www.sekab.com/chemistry/ethyl-acetate/ (accessed June 2019).

Journal Pre-proof

Journal Pre-proof

Figure 1 – Photos of crushed (left) and ground (right) leaves of *Vitis vinifera* L.

Figure 2 - Scheme of the lab-scale extraction unit – modified from [41,42].

Figure 3 - Total yield (top) and individual yields (bottom) for the extracts produced from vine leaves by Soxhlet extraction with dichloromethane (DCM), ethyl acetate (EA) and ethanol (E).

Figure 4 - Experimental SFE data (points) and modelling results (lines; BICM) for the total extraction yield. Operating conditions in Table 2.

Figure 5 - Experimental SFE data (points) and fitted BICM curves (lines) for the specific yield of LCAA (top) and triterpenes (bottom) from vine leaves. Operating conditions in Table 2.

Figure 6 - Experimental SFE data (points) and fitted BICM curves (lines) for the specific yield of sterols (top) and tocopherols (bottom) from vine leaves. Operating conditions in Table 2.

Figure 7 - Selectivity towards target compounds/families of extractives calculated for the cumulative extracts of the SFE curves.

Figure SM1 - Experimental SFE data (points) for the total extraction yield plotted against the mass of spent fluid (supercritical solvent) over the mass of used raw material.

Journal Pre-proof